Fracture Behavior of Die-Drawn Toughened Polypropylenes

J. Mohanraj,[1] N. Chapleau,[2] A. Ajji,[2] R. A. Duckett,[1] I. M. Ward[1]

[1]*IRC in Polymer Science andTechnology, Department of Physics & Astronomy, University of Leeds, Leeds, UK*
[2]*IMI-NRC 75, de Mortagne, Boucherville, Québec, Canada*

Received 20 May 2002; accepted 25 June 2002
Published online 19 February 2003 in Wiley InterScience (www.interscience.wiley.com). DOI 10.1002/app.11835

ABSTRACT: The Leeds die-drawing process has been used to make oriented sheets of toughened polypropylenes. Die-drawn oriented sheets were produced by drawing at 110°C to draw ratios of 4, 6, and 10. Comparative measurements have been undertaken of the plane stress fracture toughness at room temperature using the essential work of fracture method for isotropic and oriented polypropylene homopolymer and the two polypropylene blends containing 10 and 25% of a polyethylene-based elastomer. In the isotropic state, the blend containing 25% elastomer exhibited higher fracture toughness than the homopolymer and the 10% blend. The oriented sheets were tested both parallel (cracks perpendicular to the draw direction) and perpendicular (cracks parallel to the draw direction). For the latter case of cracks parallel to the draw direction, the fracture toughness of all the materials decreased with increasing draw ratio and up to a draw ratio of 4 the 25% blend exhibited higher fracture toughness than the other two materials. At higher draw ratios, however, the unfilled polypropylene was tougher than the blends. When tested parallel to the draw direction, all three materials failed with the cracks growing slowly initially followed by sudden rupture. © 2003 Wiley Periodicals, Inc. J Appl Polym Sci 88: 1336–1345, 2003

Key words: essential work of fracture; die-drawing; polypropylene blends; oriented polymers

INTRODUCTION

The research described here forms part of an extensive Joint Research Project between IMI Boucherville, Quebec, Canada, and the IRC in Polymer Science and Technology, University of Leeds, UK. The research project is a comparative study of the production and properties of oriented polymer sheets produced by either roller drawing (IMI) or die-drawing (IRC), and includes homopolymers and specially toughened blends of polypropylene and PET. It is well known that considerable enhancement of some properties such as stiffness and strength can be produced by solid-state molecular orientation,[1] and both roller drawing and die-drawing have been extensively explored by the present authors.[2,3] Orientation can also have a down side, especially with regard to a reduction in strength for directions other than the principal draw direction. For this reason there is particular interest in studying the fracture behavior of toughened grades, in this case for polypropylene blends containing 10 and 25% of a polyethylene-based elastomer. It is well known that by dispersing moderate amounts of the well-defined elastomer phase in the polymer matrix the toughness can be significantly improved.[4] An accepted view on the role of the elastomer particles is that these inclusions alter the stress state in the material and induce extensive plastic deformation in the matrix, by the way of multiple crazing, shear yielding of the matrix with rubber particles stretching or tearing and debonding.[4,5] The objective of the present work is to study the effect of such toughening on the fracture behavior of oriented polypropylene obtained from the die-drawing process.

The fracture characteristics of polymers exhibiting brittle fracture can be determined by using Linear Elastic Fracture Mechanics (LEFM) concepts for which the procedures are standardized.[6,7] Brittle fracture is favored by plane strain conditions that ensure that there is no plastic flow at the tip of the crack and the plastic zone remains elastic. The critical stress intensity factor, K_C, and the critical strain energy release rate, G_C, have been used to characterize the plane strain fracture. However, for ductile fracture considerable energy is dissipated in the material creating extensive plasticity ahead of the crack tip. Thus, LEFM can no longer be used to characterize this kind of fracture. For ductile fracture, two approaches initially developed for metals have now been adopted for studying the fracture behavior of polymers, namely the J integral and the Essential Work of Fracture (EWF) methodologies. The determination of fracture toughness of ductile polymers by using the J-integral

Correspondence to: I. M. Ward (I.M.Ward@leeds.ac.uk).
Contract grant sponsor: National Research Council and British Council, Canada.

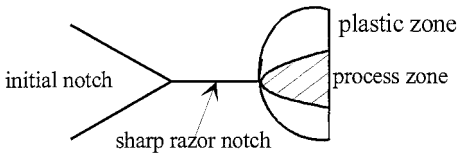

Figure 1 Schematic of process and plastic zone during the ductile fracture.

concepts originally developed for metals is now considered to be ambiguous.[8,9] In this study we have successfully used the EWF approach to determine the fracture toughness of isotropic and oriented polypropylene blends.

Essential work of fracture

The EWF concept stems from the idea originally proposed by Broberg[10] and later developed by Mai and Cottrell for thin metal sheets.[11] Owing to its experimental simplicity, this idea has now been widely acclaimed to characterize the fracture toughness of ductile and tough polymers (e.g., refs. 12–28). According to this theory,[29] the region ahead of the sharp notch can be divided into two zones: the fracture process zone, and the plastic zone. The process zone is where the crack propagates and the plastic zone encompasses the process zone (Fig. 1).

The total work required to fracture a notched specimen (W_F) is composed of two parts; the essential work of fracture (W_E), and the plastic work of fracture (W_P). W_E is the energy required to propagate the crack in the process zone and thus for the generation of new surfaces. W_E is therefore a function of the area of the ligament (a two-dimensional quantity). W_P is the energy that is dissipated in the plastic zone, and thus is a function of the volume of the process zone (a three-dimensional quantity). W_P is dependent on the size of the ligament available before fracture.

$$W_F = W_E + W_P \tag{1}$$

Rewriting the above equation in terms of specific quantities, w_E and w_P yields,

$$W_F = w_E\, lt + w_P\, \beta l^2 t \tag{2}$$

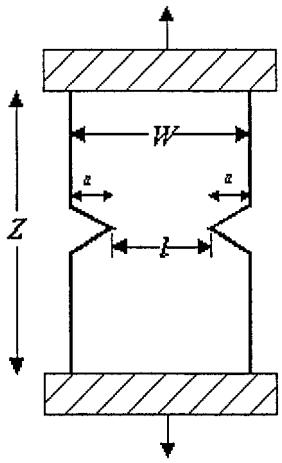

Figure 3 Geometry of the DENT specimens used in this study.

where

l is the length of the ligament (width of the sample—crack length), t is the thickness of the sample, and β is the shape factor that depends on the geometry of the process zone.

$$w_F = \frac{W_F}{lt} = w_E + \beta w_P \cdot l \tag{3}$$

The above equation indicates a linear relationship between w_F and l. From the plot, w_E (intercept of y-axis) and w_P (slope of the regression line, provided the shape of the plastic zone is well defined) can be estimated. For a given thickness, w_E is an estimate of the plane stress fracture toughness of the material independent of the specimen geometry and loading configuration.[30] To ensure that the plane stress conditions prevail during the test, ESIS (European Structural Integrity Society) suggested two exclusion limits for the ligament lengths. According to the ESIS EWF protocol,[31] the ligament length should be greater than a lower limit of three to five times the thickness of the sample i.e., $l \approx (3\text{–}5)\, t$. This constraint is to ensure that the sample is tested under plane stress conditions, which is a prerequisite for the EWF method. For samples with ligament lengths less than l_{min}, the constraint increases and the samples usually fail under mixed

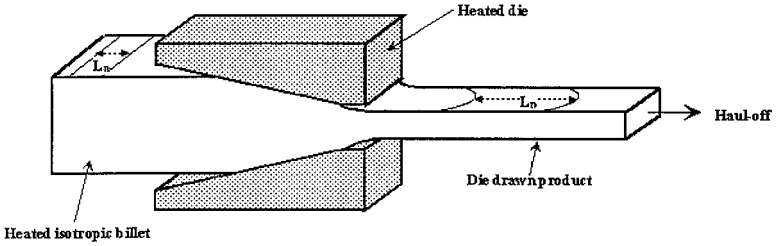

Figure 2 Schematic sketch of the die-drawing process.

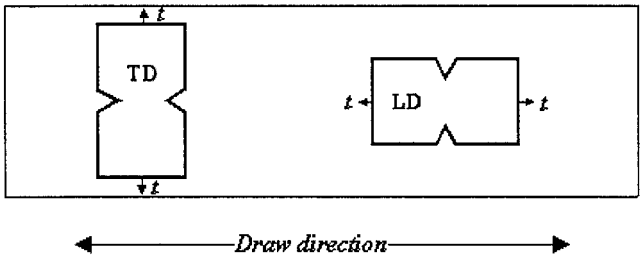

Figure 4 Schematic diagram showing the orientation of the DENT specimen with respect to the draw direction (TD—perpendicular to the draw direction, LD—parallel to the draw direction, and *t*—test direction).

mode conditions. The maximum ligament length should be kept below one-third of the width of the sample ($W/3$) to avoid edge effects, i.e., $l \approx W/3$.

EXPERIMENTAL

Materials

The fracture toughness of three materials was determined in this study. They are *A*—polypropylene homopolymer, *B*—90% polypropylene and 10% by weight elastomer, and *C*—75% polypropylene and 25% by weight elastomer. The polypropylene used in this study was a commercial grade polypropylene, Profax 6823 from Montell with a melt flow index = 0.5. The elastomer was Engage 8150, manufactured by Dow DuPont. Engage 8150 elastomer is an ethylene octene copolymer containing 25% octene. An investigation into the effect of octene content on the thermal behavior of ethylene–octene copolymer[32] has revealed that increasing the octene content beyond 20% hindered polyethylene from crystallizing and concluded that only slight traces of polyethylene crystals could be found. Both materials were supplied in the form of pellets. The blends were compounded in a corotating twin-screw extruder, at 200°C and 200 rpm, and pelletized.

Die drawing

For die-drawing, sheets approximately 5-mm thick and 100-mm wide were extruded at 200°C. On each sheet, a tag of 1-mm thick, 50-mm long, and a taper of 15° semiangle were machined to aid the start up procedure for the die-drawing process. On the wide face of each billet, lines of 20-mm spacing were drawn perpendicular to the stretch direction along the length of the sheet. The ratio of the spacing before (L_B) and after drawing (L_D) yielded the actual draw ratio, R_A.

The billet was placed in the heated chamber at 110°C and the tag gripped by the haul-off unit. The material was allowed to soak at the draw temperature for 1 h to establish thermal equilibrium. After the soaking period, the tag was drawn at a slow speed of 50 mm/min until the starting face was fully drawn out and oriented material emerged. At this point the drawing process was stopped and the tag was cut off. The product was regripped and the drawing restarted. A schematic sketch of the die-drawing process is shown in the Figure 2. For this study, *A*, *B*, and *C* were drawn to three different draw ratios, of 4, 6, and 10, by changing the haul off speed from 100 to 540 mm/min.

Fracture tests

The fracture tests were carried out in accordance with the ESIS protocol.[31] Double edge- notched tensile (DENT) specimens (Fig. 3) of nominal dimensions 90 by 25 mm were stamped from the sheets using a

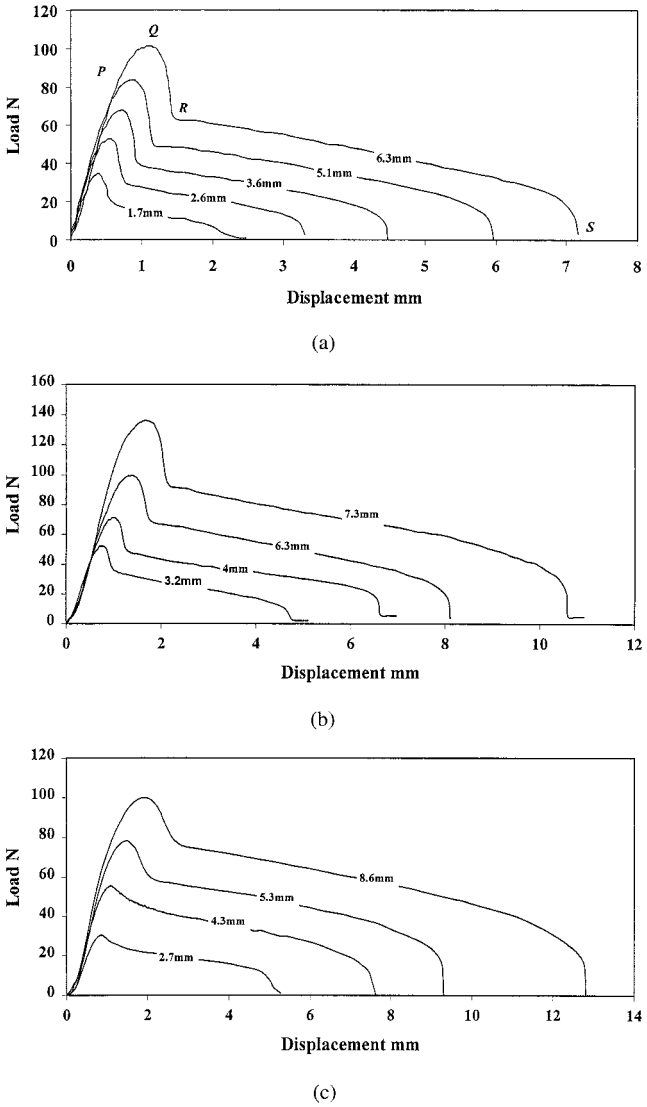

Figure 5 DENT load–displacement curves for material (a) *A*, (b) *B*, (c) *C*, with different ligament lengths. All the samples had a gauge length of 30 mm, and were tested at a crosshead speed of 10 mm/min.

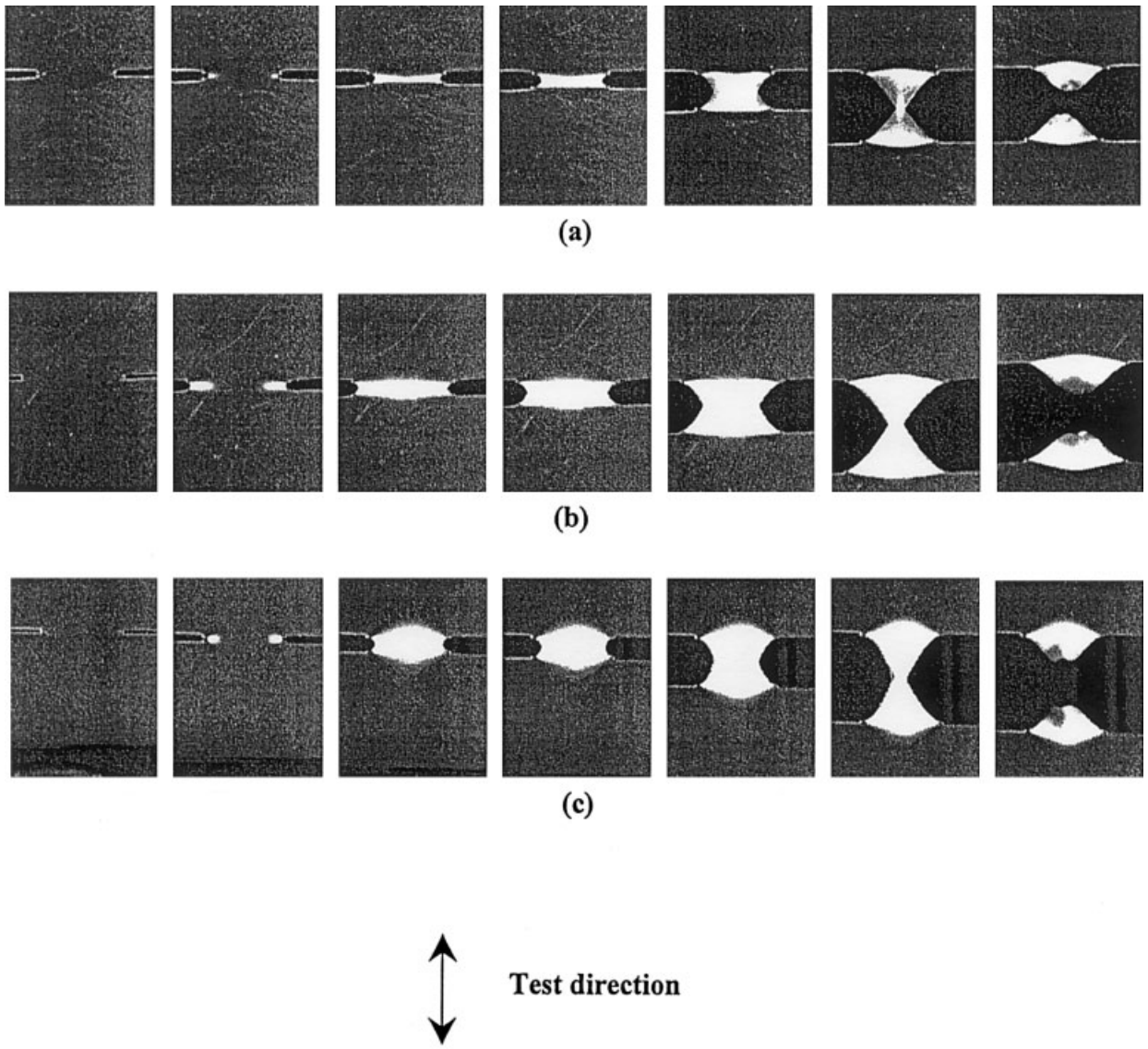

Figure 6 Photographs taken during the DENT fracture test showing ligament yielding and the instant just before final rupture for (a) *A*, (b) *B*, and (c) *C*.

standard cutter. For fracture tests on isotropic samples, pellets were compression moulded in a press at 200°C and followed by free annealing the compression moulded sheets at 120°C for 1 h to remove the orientation effects during the molding process. Specimens from the oriented sheets were cut in both the directions—along (LD) and perpendicular to the draw direction (TD) as shown in Figure 4.

Initial notches were made by using a slitting saw and the root tips were sharpened by pressing a fresh razor blade into the tip. At least 10 samples from each set were notched to give ligament lengths varying between 1.5 and 8 mm. All the samples were tested until final fracture in an Instron testing machine at a crosshead speed of 10 mm/min. The load displacement curves were recorded and the area under the curve was integrated to obtain the energy absorbed during the fracture process. A series of *in situ* pictures of the ligament was taken during the fracture test using a video camera interfaced with a computer. The ligament lengths were measured after the tests using a travelling microscope.

RESULTS AND DISCUSSION

Isotropic *A*, *B*, and *C*

The load displacement curves during DENT tests on sample *A*, *B*, and *C* as a function of ligament lengths are shown in Figure 5(a), (b) and (c) and the photographs taken during the DENT test are shown in Figure 6(a), 6(b), and 6(c). At first there is a linear elastic region up to point P [see Fig. 5(a)]. On further loading, two plastic zones were generated at the tip of

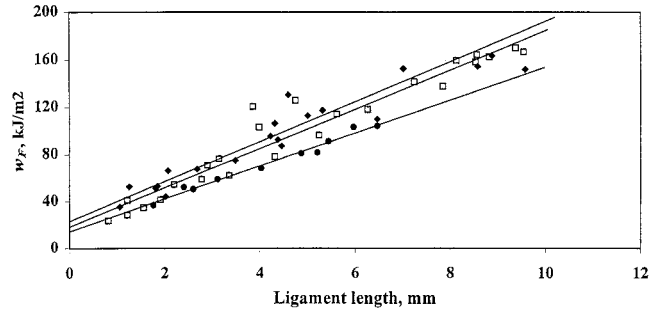

Figure 7 Specific total work of fracture versus ligament length for isotropic *A*, *B*, and *C*.

both the cracks, the size of which increased on further loading. The load eventually reached a maximum value [point Q in Fig. 5(a)] at a point when the two plastic zones met each other. The sudden drop in load after point Q indicates the necking of the yielded ligament. After complete necking of the ligament [point R in Fig. 5(a)], the cracks started to grow in a stable manner until final fracture of the specimen [point S in Fig. 5(a)]. For all the three materials as the ligament completely yielded before the crack started to propagate, as confirmed from the load displacement plots [Fig. 5(a), (b) and (c)] and from the photographs taken during the test (Fig. 6), the prerequisite for the EWF analysis was satisfied. The specific essential work of fracture, w_E, was obtained from the linear extrapolation of total work of fracture (w_F) against the ligament length (Fig. 7). The slope of the w_E vs. ligament plot gave the nonessential work of fracture or plastic work, βw_P. The effect of dimensions (thickness, width, and gauge length), geometry, and test rate on the w_E and βw_P values was undertaken in a separate study.[33] It was found from the initial study that the plane stress fracture toughness (w_E), for a particular thickness, is geometry and dimension independent provided that the plane stress conditions were maintained. This observation is in agreement with the previous studies by other workers on a wide range of amorphous and semicrystalline polymeric systems [e.g., refs. 13, 22–28]. The essential work of fracture results from Figure 7 are summarized in Table I. From the values listed in Table I, it is clear that the plane stress fracture toughness, w_E, is higher for the blends and increases with the elastomer content. The plastic work, which is the energy dissipated in the process zone, also increased with increasing elastomer content confirming that more energy is absorbed during the fracture process for the blends. It is clear from the photographs taken during the test just before complete failure (Fig. 6) that the size of the plastic zone and extension to break increases with increasing elastomer content.

TABLE I
Essential Work of Fracture Results for Isotropic *A*, *B*, and *C*

Material	w_E (kJ/m^2)	βw_P (MJ/m^3)
A (PP)	14.37 ± 0.75	13.97 ± 0.69
B (90%PP & 10%elastomer)	18.52 ± 1.93	16.62 ± 0.91
C (75%PP & 25% elastomer)	23.2 ± 2.77	16.92 ± 1.21

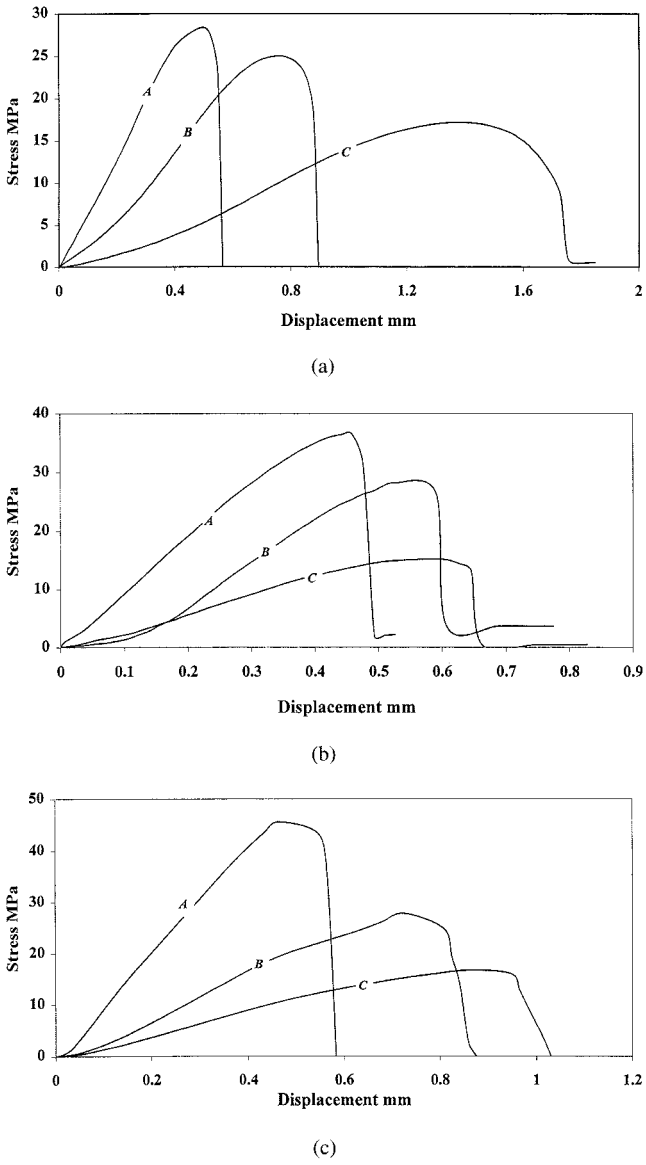

Figure 8 Stress–displacement plot for *A*, *B*, and *C* at draw ratios (a) 4, (b) 6, and (c) 10. All the samples were tested at a crosshead speed of 10mm/min.

Testing the oriented sheets in the transverse direction

The stress–displacement plots for the DENT specimens tested with the notch parallel to the draw direction for draw ratios 4, 6, and 10 are shown in Figure 8(a), (b) and (c). The plots were normalized for the

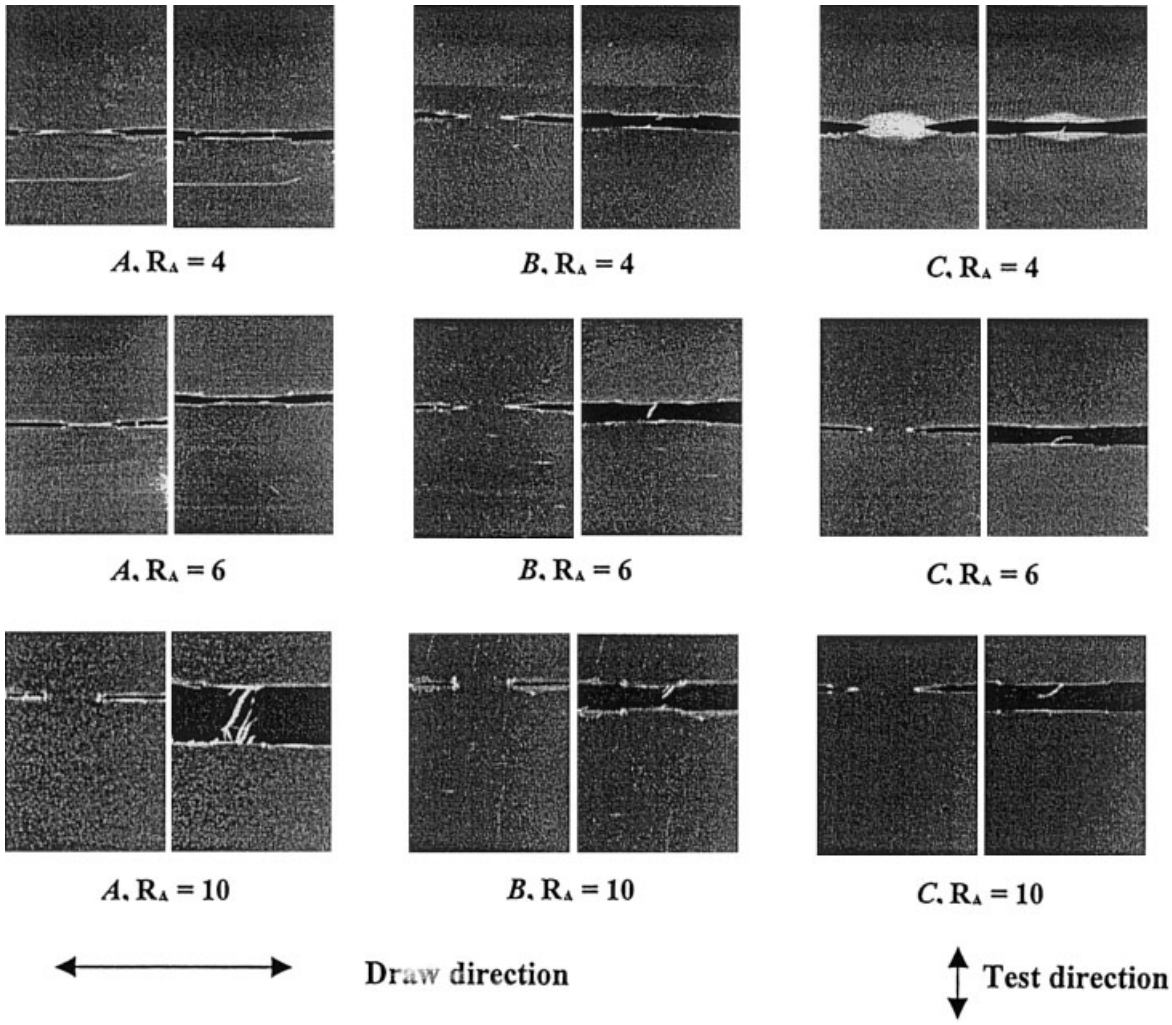

Figure 9 Photographs taken during the DENT test for draw ratios 4, 6, and 10 for samples *A*, *B*, and *C* when the cracks were sent parallel to the draw direction. The photographs were taken during the test showing ligament yielding before crack propagation and after the ligament had fully ruptured.

ligament area to account for the variation in thickness. For draw ratios 4 and 6, the ligament yielded completely before the crack travelled unstably through the sample as confirmed from the photographs taken during the test, just before crack initiation and final fracture (Fig. 9). Because the ligament yielded before final brittle fracture, the EWF method was still valid when testing along this direction. For draw ratio 10, the ligament did not yield completely before crack propagation and thus the EWF method is not valid. But the data was still analyzed for comparative purposes. The plot of the total work of fracture against the ligament length is shown in Figure 10(a), (b), and (c) for *A*, *B*, and *C* at different draw ratios. The essential work of fracture parameters obtained from Figure 10(a), (b), and (c) are tabulated in Table II.

The effect of draw ratio on the transverse fracture toughness is shown in Figure 11. As can be seen from the Figure 11 and from the results summarized in Table II, for draw ratios less than 4, *C* had higher toughness than *A* and *B*. However, for draw ratios greater than 4, *A* was tougher in the transverse direction than the blends, *B* and *C*. For sample *C* at $R_A = 4$, a large plastic zone was observed around the fracture process zone (refer Fig. 9). This observation suggests that a considerable amount of energy is being dissipated in the plastic zone, which increases the nonessential work of fracture (refer Fig. 9 and Table II) and the extension to break. As a consequence of the rise in non essential work of fracture (βw_p), the fracture toughness of *C* is considerably higher than *A* and *B* at lower draw ratios. Thus, at lower draw ratios, although the blends have reduced yield stress when compared to the homopolymers [Fig. 8(a)], the increase in extension to break is the decisive influence on the toughness of the sample.

For draw ratios greater than 4, a plastic zone can still be noticed ahead of the crack tip for the blends *B* and *C*, as shown in the *in situ* photographs (Fig. 9).

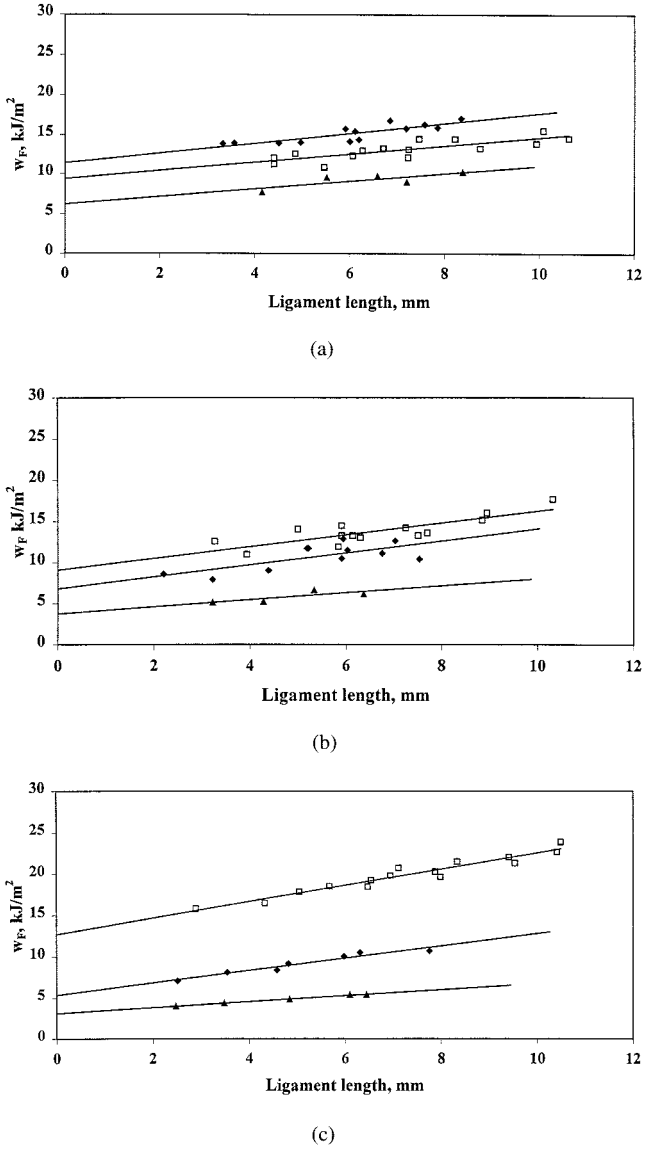

Figure 10 Specific total work of fracture vs. ligament length at draw ratios 4 (□), 6 (◆), and 10 (▲) for (a) *A*, (b) *B*, and (c) *C*. The samples were tested perpendicular to the draw direction at a crosshead speed of 10 mm/min.

This crack tip blunting mechanism, because of the energy dissipation, increased the elongation to break of the blends to higher strain. However, the considerable reduction in yield stress when compared with that of the polypropylene homopolymer reduced the toughness of the blends [Fig. 8(b) and (c)]. Structural studies are presently being performed to clarify the reduction in yield stress that resulted in a sharp fall in toughness of the blends.

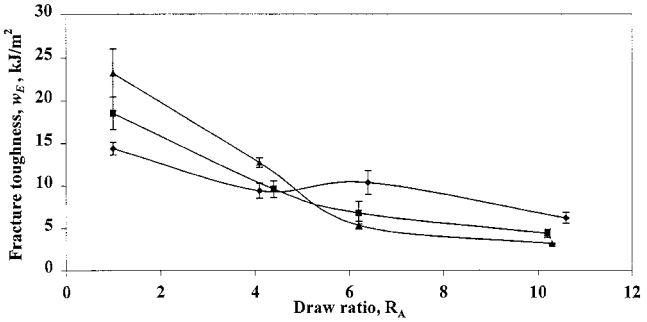

Figure 11 The effect of draw ratio on the transverse plane stress fracture toughness for *A* (◆), *B* (■), and *C* (▲).

Testing the oriented sheets in the longitudinal direction

The stress–displacement plots during the DENT test for oriented *A*, *B*, and *C* with the initial notch perpendicular to the orientation direction for draw ratios 4, 6, and 10 are shown in Figure 12(a), (b), and (c). All the specimens exhibited dual fracture behavior, which is apparent from the shape of the stress–displacement plot. The cracks initially started off slowly and during this phase the energy was continuously being accumulated in the system. After the energy reached a threshold limit, this energy was used to propagate rapidly the crack across the sample. Careful examination of the postmortem fracture surface reveals the clear distinction between the region of slow crack growth and the fast fracture (Fig. 13). The slow crack growth region appeared glossy and faint stress whitening with striations was noticed in the fast crack growth region. Because of this dual mode fracture behavior, the EWF method was not applied for this set of samples and the results have been interpreted only qualitatively for comparison purposes.

At draw ratio 4, for all the three materials, plastic zones were noticed ahead of the crack tip (Fig. 14) implying that the energy was continuously dissipated in the plastic zone as the crack traversed stably

TABLE II
Essential Work of Fracture Results Perpendicular to the Draw Direction for *A*, *B*, and *C* at Draw Ratios 4, 6, and 10

	$R_A = 4$		$R_A = 6$		$R_A = 10$	
Material	w_E (kJ/m^2)	βw_P (MJ/m^3)	w_E (kJ/m^2)	βw_P (MJ/m^3)	w_E (kJ/m^2)	βw_P (MJ/m^3)
A	9.39 ± 0.5	0.53 ± 0.12	11.42 ± 0.77	0.63 ± 0.14	6.21 ± 0.85	0.48 ± 0.21
B	9.07 ± 0.63	0.71 ± 0.14	6.79 ± 0.67	0.73 ± 0.24	3.77 ± 0.83	0.42 ± 0.24
C	12.71 ± 0.55	0.99 ± 0.07	5.35 ± 0.47	0.75 ± 0.09	3.15 ± 0.08	0.36 ± 0.02

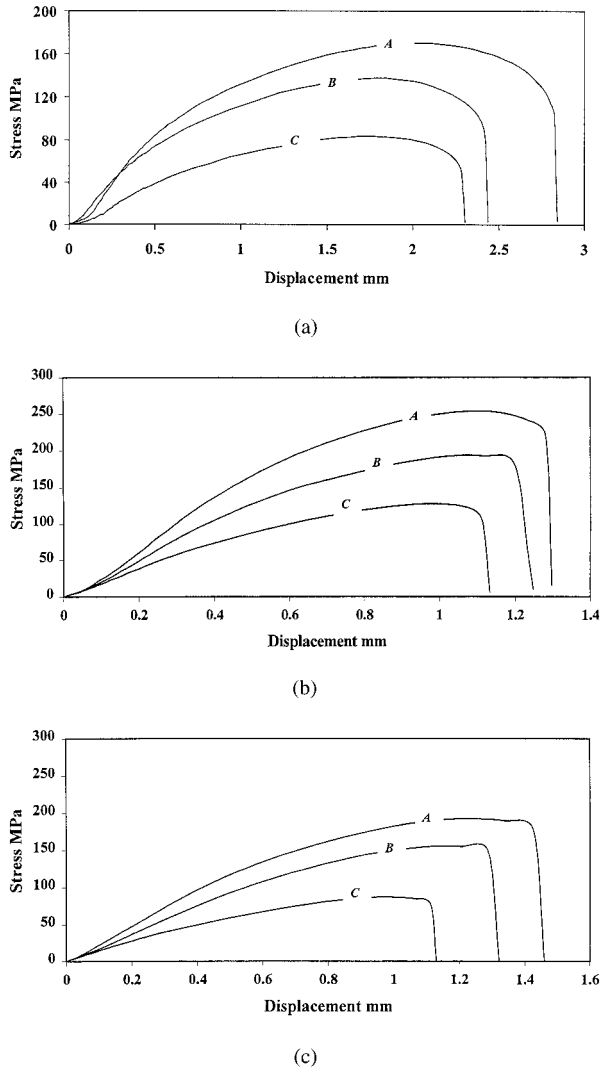

Figure 12 Stress–displacement plot for *A*, *B*, and *C* at draw ratios (a) 4, (b) 6, and (c) 10. All the samples were tested at a crosshead speed of 10 mm/min.

through it. Because of the overlapping of the yielding and the slow crack growth phenomenon, the initial part of the stress displacement plot at draw ratio 4 is highly curved when compared with that of the plots at higher ratios. However, for draw ratios 6 and 10, no plastic zone was noticed ahead of the crack tip (Fig. 14). At this juncture, also of particular interest is the shape of the crack tip at different draw ratios. At lower draw ratios the crack tip appeared blunter and at high draw ratios the crack tips were sharper.

With increasing draw ratio the intrinsic stress–strain behavior (measured in tension on unnotched samples) changes in a number of ways. The elastic modulus and yield stress in the draw direction increase markedly with increasing draw ratio. In addition, the stress–strain curve beyond yield generally shows enhanced strain hardening and reduced ductility. We now consider the implications of these observations for the present fracture experiments.

At the crack tip there is a competition between plastic deformation and rupture. At low draw ratios, the yield stress is lower than the crack opening stress, there is some ductility, and thus the sample yields and deforms much further before fracture. At high draw ratios, the yield stress and the strain hardening have become so high that the fracture intervenes, either before or shortly after yielding, and there is no evidence of plastic flow at the crack tip. The crack opening stress is now below or quite close to the yield stress.

Comparing the area under the stress–displacement plot for the same ligament length for *A*, *B*, and *C*, two conclusions can be made. First, for all the three materials, the fracture energy increased with increasing draw ratio. Second, for a particular draw ratio, the homopolymer *A* had higher fracture energy than the blends *B* and *C*.

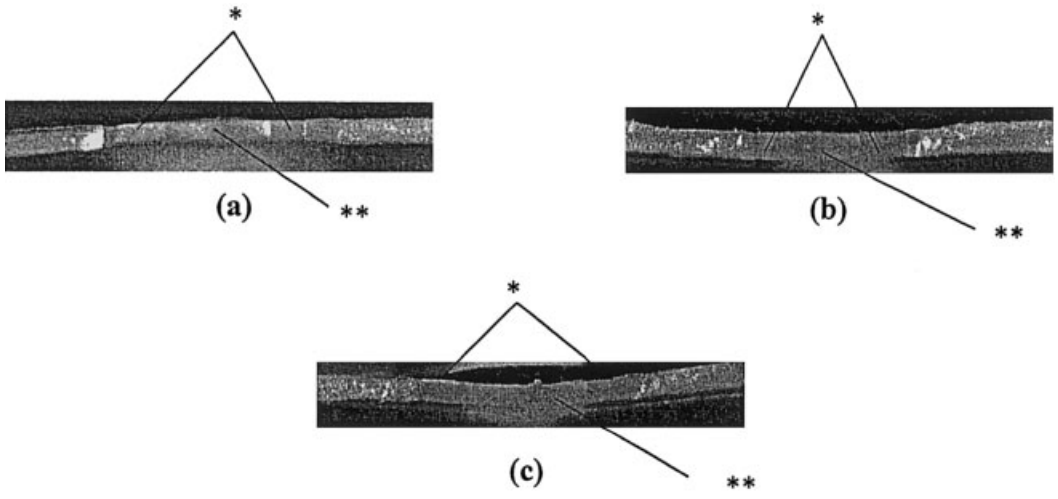

Figure 13 Fracture surface of the oriented (a) *A*, (b) *B* and (c) *C*, when tested perpendicular to the draw direction showing the slow crack growth region (*) and the unstable rupture region (**).

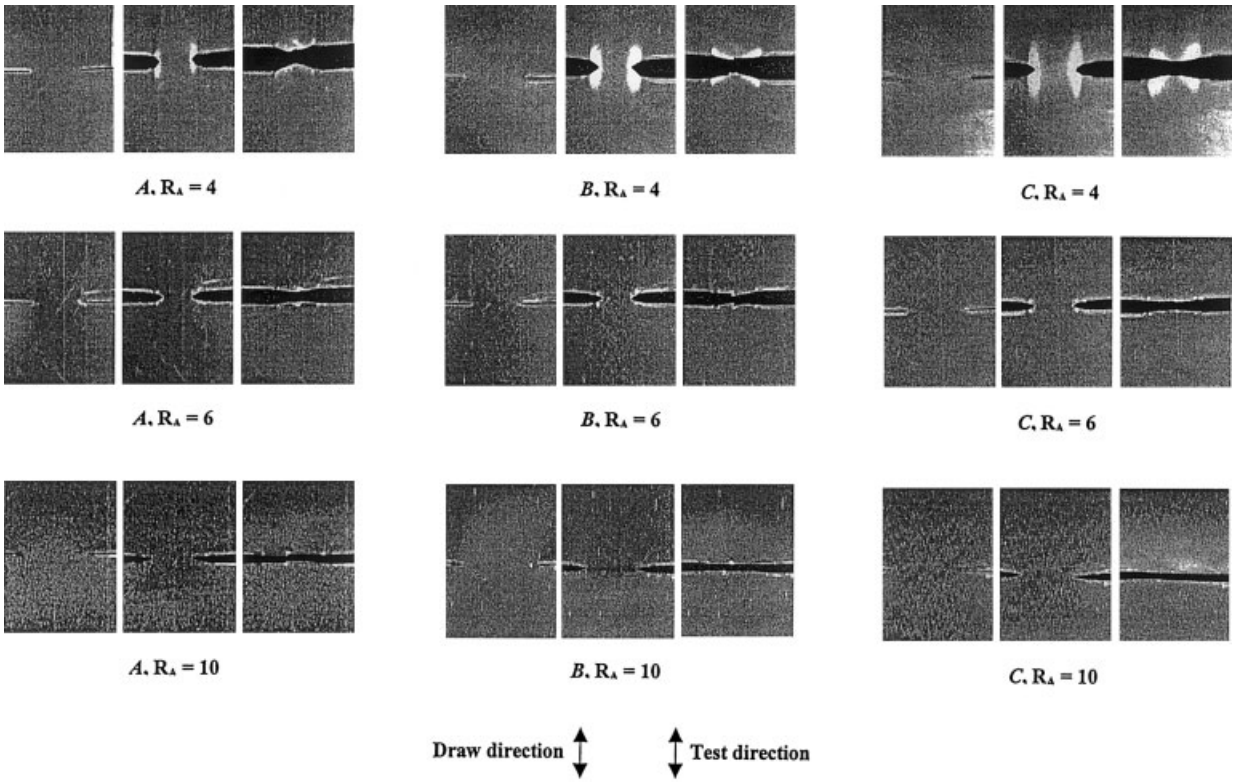

Figure 14 Photographs taken during the DENT test on for *A*, *B*, and *C* draw ratio 4, 6, and 10 samples when tested in the longitudinal direction. Photographs show the sample before test, stable crack growth, and after final brittle fracture.

Polypropylene in its isotropic form has a spherulitic morphology composed of crystalline and noncrystalline components. On orientation, the spherulitic structure is destroyed and the cleaved crystals are restacked into newly formed microfibrils. The microfibrils are composed of alternating chain folded crystalline blocks connected by taut tie molecules.[34] The degree of crystalline orientation and the tautness of the tie molecules increase with draw ratio. It has been reported earlier that the increase in crystalline orientation and the generation of more taut tie molecules contributed to the increase in stiffness, strength, impact fracture toughness, and creep resistance along the draw direction.[35–38] It was confirmed from the WAXS data that *A* had higher crystalline orientation than the blends *B* and *C*[33] because the inclusion of a rubbery phase reduces the degree of crystalline orientation in polypropylene and inhibits the formation of fibrillar morphology.

CONCLUSIONS

The fracture toughness of isotropic and oriented polypropylene and blends of polypropylene with a polyethylene-based elastomer was studied by the essential work of fracture method by using the double-edge notch tension test at quasi-static loading rates. For isotropic samples, the specific essential and nonessential work of fracture increased with increasing elastomer content in the polypropylene. When the oriented samples were tested in the transverse direction, up to a draw ratio of 4, the blend containing 25% elastomer was tougher than the blend containing 10% elastomer and the polypropylene homopolymer. At draw ratios greater than 4, the scenario was totally different with the polypropylene homopolymer exhibiting higher toughness than the blends. In the longitudinal direction, the fracture toughness of polypropylene and the blends increased with draw ratio. For a particular draw ratio, the unmodified polypropylene exhibited higher fracture energy than the blends.

J. Mohanraj is grateful to Overseas Research Student Awards scheme, UK, for a Postgraduate research scholarship award.

References

1. Coates, P. D.; Ward, I. M. Polymer 1979, 20, 1553.
2. Richardson, A.; Parsons, B.; Ward, I. M. Plas Rubber Proc Appl 1986, 6, 347.
3. Ajji, A.; Cole, K. C.; Dumoulin, M. M.; Ward, I. M. Polym Eng Sci 1997, 37, 1801.
4. Bucknall, C. B. Toughened Plastics; Applied Science: London, 1977.
5. Wu, J.; Mai, Y. W. Mater Forum 1995, 19, 181.

6. Williams, J. G.; Cawood, M. J. Polym Testing 1990, 9, 15.
7. ISO 13586:2000(E), Plastics—Determination of Fracture Toughness (GIC and KIC)—Linear Elastic Fracture Mechanics (LEFM) Approach (2000).
8. Narisawa, I.; Takemori, M. T. Polym Eng Sci 1989, 29, 671.
9. Huang, D. D.; Williams, J. G. J Mater Sci 1987, 22, 2503.
10. Broberg, K. B. In Proceedings of an International conference on Fracture Mechanics and Technology, Hong Kong, March 1977; Sih, G. C.; Chow, C. L., Eds.; Sijthoff & Noordhoff International: The Netherlands, 1977.
11. Mai, Y. W.; Cotterell, B. J Mater Sci 1980, 15, 2296.
12. Hashemi, S. J Mater Sci 1997, 32, 1563.
13. Arkhireyeva, A; Hashemi, S. Plas Rubber Comp 2001, 30, 337.
14. Mai, Y. W.; Powell, P. J Polym Sci Part B Polym Phys 1991, 29, 785.
15. Wu, J.; Mai, Y. W. Polym Eng Sci 1996, 36, 2275.
16. Wu, J.; Mai, Y. W.; Cotterell, B. J Mater Sci 1993, 28, 3373.
17. Karger-Kocsis, J.; Czigany, T. Polymer 1996, 37, 2433.
18. Chan, W. Y. F.; Williams, J. G. Polymer 1994, 35, 1666.
19. Mouzakis, D. E.; Gahleitner, M.; Karger-Kocsis, J. J Appl Polym Sci 1998, 70, 873.
20. Li, W. D.; Li, R. K. Y.; Tjong, S. C. Polym Testing 1997, 16, 563.
21. Marchal, Y.; Oldenhove, B.; Daoust, D.; Legras, R.; Delannay, F. Polym Eng Sci 1998, 38, 2063.
22. Maspoch, M. L.; Ferrer, D.; Gordillo, A.; Santana, O. O.; Martinez, A. B. J Appl Polym Sci 1999, 73, 177.
23. Hashemi, S. Polym Eng Sci 1997, 37, 912.
24. Arkhireyeva, A.; Hashemi, S.; O'Brien, M. J Mater Sci 1999, 34, 5961.
25. Paton, C. A.; Hashemi, S. J Mater Sci 1992, 27, 2279.
26. Hashemi, S.; Yuan, Z. Plas Rubber Comp 1994, 21, 151.
27. Hashemi, S. J Mater Sci 1993, 28, 6178.
28. Maspoch, M. L.; Henault, V; Ferrer-Balas, D.; Velasco, J. I.; Santana, O. O. Polym Testing 2000, 19, 559.
29. Mai, Y. W.; Cotterell, B. Int J Fract 1986, 32, 105.
30. Mai, Y. W. Polym Commun 1989, 30, 330.
31. ESIS Test Protocol for essential work of fracture (Version 6), European Structural Integrity Society (2000).
32. Vanden Eynde, S; Mathot, V. B. F.; Koch, M. H. J.; Reynaers, H. Polymer 2000, 41, 4889.
33. Unpublished results.
34. Peterlin, A. J Mater Sci 1971, 6, 490.
35. Taraiya, A. K.; Unwin, A. P.; Ward, I. M. J Polym Sci Part B Polym Phys 1988, 26, 817.
36. Samuels, R. J. Structured Polymer Properties; John Wiley & Sons: London, 1974.
37. Duxbury, J.; Ward, I. M. J Mater Sci 1987, 22, 1215.
38. Chaffey, C. E.; Taraiya, A. K.; Ward, I. M. Polym Eng Sci 1997, 37, 1774.